17th World Conference on Earthquake Engineering, 17WCEE
Sendai, Japan - September 27th to October 2nd, 2021

DEMONSTRATING THE POTENTIAL FOR GROUND IMPROVEMENT TO REDUCE ROCKING-INDUCED SEISMIC DISPLACEMENTS

J.T. Newgard[(1)], T.C. Hutchinson[(2)], J.S. McCartney[(3)]

[(1)] *Research Assistant, Structural Engineering, UC San Diego, jnewgard@eng.ucsd.edu*
[(2)] *Professor, Structural Engineering, UC San Diego, tahutchinson@eng.ucsd.edu*
[(3)] *Professor, Structural Engineering, UC San Diego, mccartney@eng.ucsd.edu*

Abstract

Incremental improvements in the seismic design of structures have largely revolved around recognizing the importance of ductility and predictable yielding – yet there remains an untapped source of these critical mechanisms in the form of controlled hinging in foundation soils. However, to effectively induce rocking during an earthquake and harness enhanced energy dissipation in foundation soils, the foundation must be under-designed or sized smaller such that it has a low to moderate factor of safety against bearing failure. A consequence of their energy dissipation capability is that rocking foundations may exhibit undesirable deformations during and following shaking, including large transient rotations and residual settlements. This study seeks to understand how strategic improvement of the soils beneath these footings can be used to reduce rocking-induced seismic displacements. To this end, a numerical model in the OpenSees platform was assembled to demonstrate the potential for ground improvement to control the kinematics of rocking footings. The model was first evaluated using results from a suite of centrifuge experiments conducted at UC Davis that involved shake table tests on a spread footing embedded in medium loose dry sand that was reinforced by soil-cement columns. The model was then extended to conduct a parametric evaluation, varying the safety factor against bearing failure between 2-10 by changing the quantity and spatial distribution of the improvement columns. Results from the numerical simulations, and in particular the cross-comparison of response results amongst improved and unimproved base soils, were then used to inform the design of a centrifuge-scale testing program to be conducted at UC San Diego. This testing program will be geared around 1) resolving the appropriate level of ground improvement to balance enhanced energy dissipation and acceptable residual settlement and 2) providing additional data for validation of the OpenSees model.

Keywords: ground improvement; rocking; spread footing; earthquake; numerical modeling

1. Introduction

Rocking columns are a natural choice to pair with a shallow foundation that dissipates energy because the hinged connections to the superstructure in a rocking column do not transmit the excess moments that a traditional fixed column, fixed base design does. Although several studies have been performed on rocking column bridge structures, the energy dissipation is almost universally assumed/designed to occur through structural elements [1, 2]. Unique structural elements have been proposed to dissipate energy such as springs inside the columns [1] or special bearings between the columns, deck, and abutments [2]. Although it is well understood that energy dissipation can reduce damage to the structure, this may come at a high cost to the overall project initially and for repairs after an earthquake. Although using the foundation soil to dissipate energy may be more cost effective, relatively few studies have been investigated this topic. This stands in contrast to typical design practice specified in the California Seismic Design Criteria where the foundation remains elastic (fixed base) and the plastic hinge develops in the column (typically near to the top and/or bottom of the column). Indeed, the California Bridge Seismic Retrofit Program most often aims to make shallow footings even more rigid by deploying tiedown anchors, micropiles, and post-grouted piles to underpin the footings and resist uplift loads [6].

A shallow footing will tend to rock when the column height is relatively large compared to the plan area of the footing. Columns on shallow footings will typically rock when their center of mass is at least one footing length high. But a footing with a smaller area will have a lower safety factor against quasi-static bearing failure. This bearing capacity can be increased by ground improvement, which is important because the factor of safety against bearing capacity is closely linked with the residual rotations of a rocking footing [2, 3]. With this in mind, a strategy emerges wherein the footing area is reduced while improving the soil near the footing to simultaneously mobilize an acceptable factor of safety for vertical bearing capacity while encouraging the footing to rock during a seismic event. Although engineers commonly associate ground improvement with mitigating liquefaction, lateral spreading, and settlement hazards for shallow foundations, experiments dedicated specifically to rocking suggest that only shallow soil improvement is needed because rocking induced soil yielding is only mobilized within a shallow layer underneath the footing [5]. For example, placing geogrid and geocells in sand was found to increase the bearing capacity by about 2.5 times in large-scale experiments [4]. Another involved direct soil mixing of a continuous volume of alluvial sands susceptible to scour and erosion from water flows in a creek bed [7]. A cross-section of the soil mixing geometry is shown in Fig. 1.

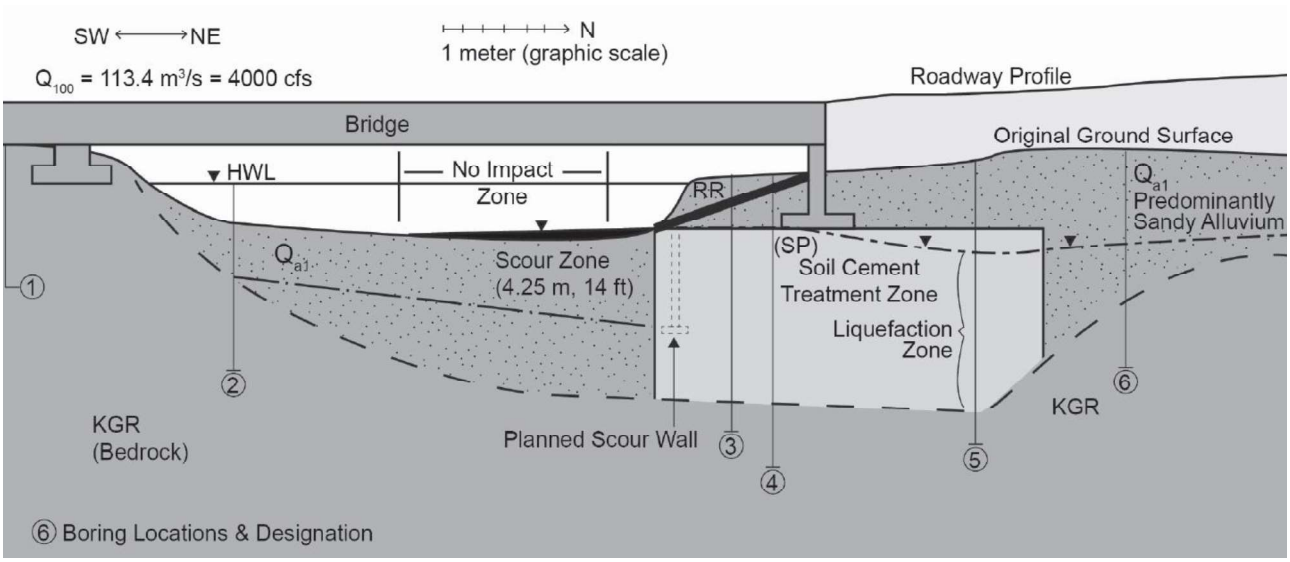

Fig. 1 – Soil cement mixed treatment zone [7]

While the mixed treatment zone was fairly large, it allowed designers to avoid a bridge founded on cast-in-drilled-hole (CIDH) piles in bedrock, where the piles would have been subject to potentially large downdrag and shear forces from liquefying and laterally spreading soils, respectively. It was estimated that the improvement saved about $1 million US over the CIDH deep foundation alternative. Another case history involved the placement of 2.44 m (8-ft) diameter cement-soil mixed columns supporting shallow foundations for a surface street bridge in Anchorage – a bridge that sustained only minor damage in the large earthquake that struck shortly after it was built [8]. The mixed columns successfully prevented any significant softening or liquefaction of surficial peat and soft silt layers, respectively.

The above two cases are provided simply to highlight the familiarity of geotechnical engineers with the myriad benefits of ground improvement in mitigating seismic hazard and reducing costs by avoiding the need for a deep foundation. This begs the question why the advancement has not been made to use ground improvement to not only support the structure, but to reduce the loads and/or displacement demands during an earthquake. The answer may be twofold: 1) relatively few studies demonstrating the potential for ground improvement to control the kinematics of a rocking footing, and 2) a lack of familiarity of practicing engineers with these same high-quality studies and case histories, introduced below.

The Rion-Antirion Bridge in Greece represents an ambitious and large-scale field example of the use of rocking shallow footings [9]. This bridge spans a major waterway and is almost 3,000 meters long with four cable-stay pylons rising over 200 m above the mudline. Each of these pylons is supported by a gravity mat, itself resting on top of about 150 to 200 inclusions consisting of 2 m-diameter, 25 m-long steel pipes driven in a 7 m grid in the soft to medium stiff mostly fine-grained alluvial sediments. Remarkably the gravity mats have no structural connection to these inclusions; the superstructure was designed to be compatible with substantial sliding of the pylons during a seismic event. This harmonious compatibility between superstructure and foundation was analyzed via a pair of macro-elements, where one each represented the near field and far field soils around the foundation. The elements together comprise a series of springs and dashpots capable of capturing the inertial forces (arising from interaction of the structure with the foundation) and kinematic forces (arising from the interaction of the foundation with incoming wave energy). Illustrations of the gravity mat and pipe inclusions are shown in Fig. 2.

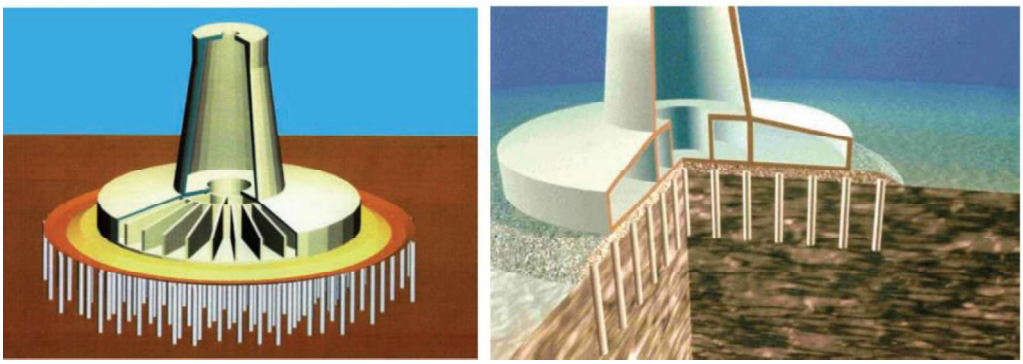

Fig. 2 – Gravity mat and pipe inclusions at Rion-Antirion Bridge [9]

By far the most comprehensive experimental studies of the rocking footing design have been conducted at UC Davis, with much of theirs (as well as other studies) contributing to the development of the Foundation Rocking in Slow-Cyclic (FoRCy) [10] and Dynamic (FoRDy) [11] experimental databases as well as providing the basis for acceptable rocking footing kinematics in design code (ASCE 41, 2017). These experimental databases are searchable by any test variable including footing dimensions, sand density and friction angle, load magnitude and bearing capacity factor of safety, and structure characteristics. The moment, rotation, settlement, and sliding data are all publicly available for download from the database.

A significant contribution to the FoRDy database [11] was made by Deng et al. [3] and Deng and Kutter [12] who reported results from a suite of centrifuge experiments performed on complete model bridge structures comparing the performance of small rocking footings against large elastic footings. The columns and bridge deck were carefully constructed to preclude these structural elements from reaching capacity before the footings – thereby ensuring the onset of rocking during the event. The structure founded on small rocking footings sustained less damage, and the residual settlement of the footings increased with increasing cumulative rotation and with increasingly heavily loaded footings.

Other studies determined that long, slender footings (along the rocking axis) tend to settle more than wide (more square) footings because the contact area of the slender footings mobilized a greater proportion of out-of-plane settlement during rocking [13, 14]. The propensity of a rocking footing to re-center itself following a seismic event has been established by analyzing a considerable variety of results in the FoRCy and FoRDy databases [15]. Only the most heavily loaded footings exhibited problematic residual rotations – medium to lightly loaded footings exhibited a natural tendency to re-center themselves.

Most relevant to the present paper's investigation of ground improvement as a means to control the kinematics of a rocking footing, was a study involving placement of four concrete columns around the perimeter of a footing as shown at the left of Fig. 3 [12]. While residual settlement of this improved footing was reduced to approximately 50%, compared with the unimproved case, the energy dissipation was correspondingly reduced as well. The energy dissipation ratio (EDR) from these tests is shown in the middle of Fig. 3, and the settlement (s) normalized by footing length (L_f) is shown at the right of Fig. 3.

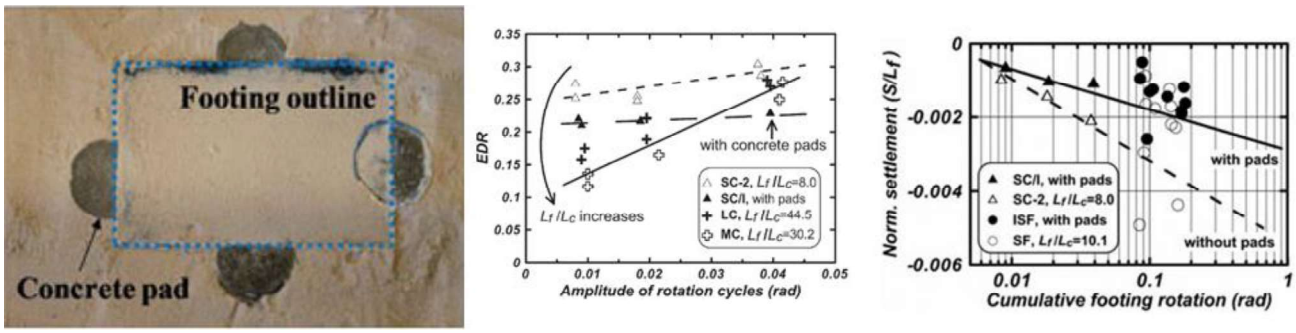

Fig. 3 – Energy dissipation and settlement of a footing resting on concrete pads [12]

Practicing engineers may be hesistant to deviate from the California Seismic Design Criteria and design smaller rocking footings; yet this hesitancy may be diminished with awareness of recent recommendations in other building codes (e.g. ASCE 41-17, Chapter 8). The allowable rotations (θ) from ASCE 41-17 at the Life Safety Performance Level are shown in Fig. 4 as a function of the moment applied (M) to a rocking footing of width (b) normalized by its moment capacity (M_c). The curves are taken from Table 8-4 in the code and reflect the fact that lightly loaded footings exhibit a stiffer moment-rotation response, and may reach larger rotations in the Acceptance Criteria. Wide footings (Fig. 4b) may reach larger rotations than narrow footings (Fig. 4a) because, as mentioned above, they exhibit less residual settlement than the narrow footings. Note the heavily loaded footing, where ½ of the total area (A_f) is needed to resist the vertical load as the footing rocks on its side, is only allowed to reach 40% of its moment capacity and rotate 3 mrad. This is due to excessive yielding that would otherwise occur for this heavily loaded footing at applied moments and rotations beyond these limits. As evident by the aforementioned field applications, experiments, and emerging design guidance, the rocking footing design has been surprisingly well-studied although as it has not been widely adopted in engineering practice. This paper aims to demonstrate how familiar ground improvement techniques can be used to ensure that a smaller rocking footing dissipates energy safely, that is, while maintaining kinematic compatibility with the rest of the structure.

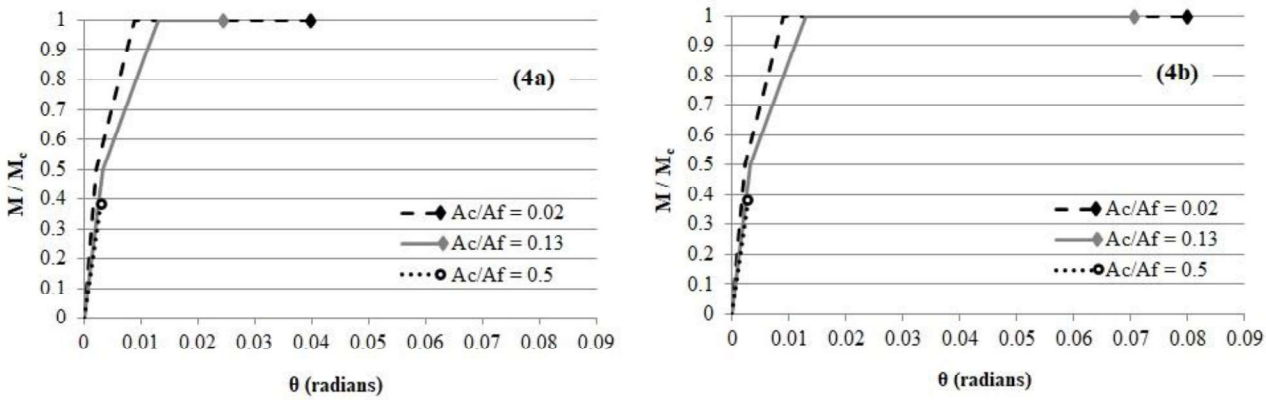

Fig. 4 – Moment-rotation curves in the Acceptance Criteria at the Life Safety Level (ASCE 41-17) a) narrow footings (b/L_c=0.3) and b) wide footings ($b/L_c \geq 10$)

2. Numerical Model Construction

The problem considered in this study involves a shallow footing resting on dry sand. The model has been constructed in the OpenSees platform and consists of two main parts: 1) the foundation soils represented by plane-strain quad elements, and 2) the footing-column structure assembly represented by elasticBeamColumn elements. Simpler quad elements were chosen over the Nine Four Node Quad u-p elements due to the absence of groundwater. The model is similar to that described by Liu et al. [16] and Liu and Hutchinson [17] in the sense that the soil-footing interface is explicitly modeled, rather than being replaced by equivalent springs [e.g. 18] or a macro-element [e.g. 19]. As in the Liu model, the footing nodes are connected to the soil surface nodes via an elastic-no-tension material interface. A new feature developed in this study is the embedment of the footing beneath the soil surface.

The model is constructed as follows. The soil quad elements are defined with the PressureDependMultiYield material model within the 2-degree-of-freedom (DOF) model builder. Prior to embedding the footing, a two-stage gravity analysis (first stage = elastic material, second stage = update to elastoplastic material) is first performed for a flat soil surface to obtain at-rest stresses in all the quad elements. Then any nodes and elements exclusively within the embedment area are effectively excavated via the remove command. Next the 3-DOF model builder is invoked and "dummy" nodes are created and tied to the 2-DOF soil surface domain via the equalDOF command. The "dummy" nodes are fixed against rotation as the soil surface nodes have no rotational or moment resistance. Finally, the elasticBeamColumn structure nodes and elements are created (still within the 3-DOF model builder) and flatSliderBearing elements connect the "dummy" nodes to these structure nodes. These slider elements are a perfect fit to capture the soil-footing interface as they allow the elastic-no-tension and Coulomb friction material models, defining the releasing and sliding behavior respectively, to be specified all in one element command. Note that each grouping of soil surface nodes, "dummy nodes", and structure nodes all have the same geometric coordinates, as both equalDOF and flatSliderBearing are types of zero-length elements. The key model commands described above are listed in Table 1 and accompanied by an illustration of the model in Fig. 5.

The command in note 1 creates a quad element with tag 1 and defined by nodes 1, 2, 3, and 4. The element has unit thickness and is of the "PlaneStrain" type with material tag 5. A body force corresponding to acceleration due to Earth's gravity of 9.81 m/s^2 is applied to all these elements to obtain correct at-rest stresses. Per correspondence with the quad element author, it is imperative that a unit thickness is specified jointly with the "PlaneStrain" type. It was observed that a thickness greater than 1 inadvertently increased the stiffness of the elements.

The command in note 2 creates a flatSliderBearing zero-length element with tag 102 between the elasticBeamColumn node 7 and the "dummy" node 5, which themselves bridge the 2-DOF soil domain and 3-DOF structure domain. Note 2a specifies the correct orientation for friction on the sides of the footing,

while note 2b specifies the same for the bottom of the footing. This is best checked by creating a single element and applying a normal (N) and horizontal (H) load to the slider to check the onset and magnitude of sliding (the analysis should fail to converge once the ratio of H/N reaches the friction coefficient, μ). The axial material models (acting perpendicular to H) listed as –P 8 and –P 7 house no-tension springs which release in the appropriate direction as a gap develops between the footing and soil during rocking. An initial stiffness (k_{init}) tangential to H of 1000 [1/m] is defined such that displacement prior to reaching H/N=μ is very small. For example, for H/N = 0.1 and k_{init}=1000 [1/m], the displacement in the horizontal direction is 0.1/1000 [1/m] = 0.0001 m = 0.1 mm. These slider elements should not have any moment capacity (listed as –Mz 10), so a uniaxial material with small stiffness is specified in material model 10. The associated friction and material models defined in these slider elements are listed as notes 4-7 below. The friction coefficient μ = 0.40 corresponds to a concrete-sand interface friction angle of 22° [20].

Table 1 – Model parts and associated commands

Illustration Type	**Model Part**	**Command Format**
———	quad element	*see note 1*
– – – – .	2-DOF to 3-DOF domain tie	equalDOF 4 5 1 2
- - - - - - - -	flatSliderBearing element	*see note 2*
▭	elasticBeamColumn element	*see note 3*
↺	rotational fixity	fix 5 0 0 1
nodes 1-4	2-DOF builder nodes	node 4 9.5 0.0
nodes 5-8	3-DOF builder nodes	node 5 9.5 0.0 node 7 9.5 0.0
nodes 9-10	2-DOF builder excavated nodes	node 9 9.5 0.2
X	node or element within excavated area	remove node 9 remove element 101

Notes:
[1] element quad 100 1 2 3 4 1.00 "PlaneStrain" 5 0.00 0.00 0.00 -9.81
[2a] element flatSliderBearing 77 9956 10042 1 1000 -P *8* -Mz *10* -orient -1 0 0 0 1 0
[2b] element flatSliderBearing 102 5 7 1 1000 -P *7* -Mz *10* -orient 0 1 0 -1 0 0
[3] element elasticBeamColumn 104 7 8 3.00 50000000.00 2.25 1
[4] frictionModel Coulomb 1 0.40
[5] uniaxialMaterial Elastic *7* *10* 0 2500000
[6] uniaxialMaterial Elastic *8* 2500000 0 10
[7] uniaxialMaterial Elastic 10 0.01

The command in note 3 creates the elasticBeamColumns representing the footing. These beam elements transfer loads imposed at the top of the structural column to the soil via the slider elements. The beam elements have been given a unit thickness [m] and a depth three times that yielding a cross-sectional area and moment of inertia of 3 m^2 and 2.25 m^4, respectively. The elastic modulus is taken as 50 GPa, sufficiently high to preclude any bending in the beam elements themselves.

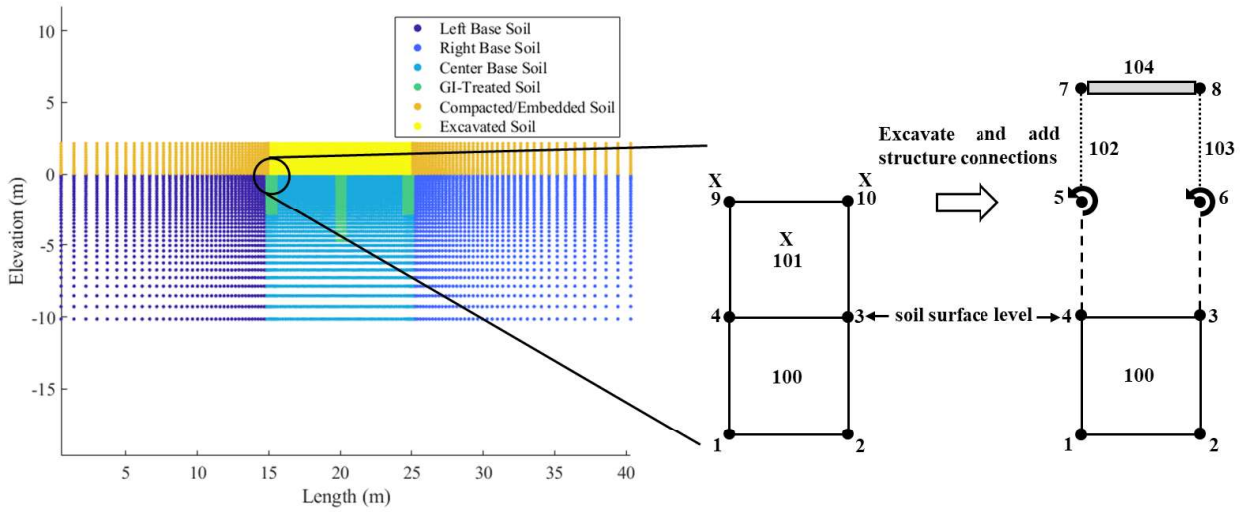

Fig. 5 – Model illustration – note node/element numbers map to those in Table 1 footnotes

3. Numerical Model Parameters, Solution Strategy, and Validation Results

The model parameters were selected for the purposes of validating slow cyclic results against those reported by [12]. In this case, however, the minimum and maximum void ratio of the Ottawa 65 sand are taken as 0.503 and 0.853 [21]. For a relative density (D_R) of 50% the void ratio is 0.68 and the initial shear modulus is approximately 80 MPa according to a relationship derived from resonant column testing [22]. The friction angle is related to the relative density via the mean confining stress [23] and dilatancy parameters [24] and was calculated by procedures detailed in [13] and reported by [12]. This results in a friction angle between 33° and 37° depending on the D_R of the sand in the test examined. In the absence of dedicated calibration testing, other soil parameters such as density, and peak shear strain and mean effective confining pressure, are taken per those suggested for the PressureDependMultiYield material for a medium dense sand [25].

Increasing the number of static analysis steps (up to 200 steps have been utilized for a half load cycle of lateral pushover) and using the energy increment test instead of the displacement increment test greatly improves convergence of the solver. The problem presents convergence issues because the structure needs to release from the soil surface, and strains are concentrated near the corners of the footing. Convergence was more likely when displacement control at the top of the column in the x-direction (DOF=1 in elasticBeamColumn elements) was used rather than in the rotation-direction (DOF=3 in elasticBeamColumn elements). Ultimately, a unique solution code was written which advances the lateral pushover one step at a time; where the displacement step size is allowed to vary, the test tolerance is sequentially relaxed as needed to ensure convergence within each step, and the slow cyclic load is reversed once the rotation at the footing's center base meets a predetermined pattern set by the user. Once convergence at a more relaxed test tolerance is achieved, the tolerance is reduced back to its original value to prevent numerical error from accumulating.

Model validation was performed on two tests in [12] for footings of 6.7 meters (SC-2) and 9.8 meters (MC) in length, both embedded 2.2 meters in medium dense sand. Three model cases are investigated, from 1) with a lateral constraint preventing the center node of the footing base from sliding in the x-direction, 2) no lateral constraint, and 3) no lateral constraint and increased shear modulus (150 MPa) for soils on the sides of the footing. Case 1 was performed because this constraint was imposed by Liu [26] who investigated a footing on the soil surface which required a robust constraint against sliding. For the present study, it has been deemed more appropriate to allow passive resistance along the sides of the embedded footing and friction along its base to resist lateral loads, rather than an artificial constraint which inevitably takes on a significant portion of applied loads. In Case 2, the footing exhibited a much higher magnitude of sliding than that observed in the test data, and so the decision was made to artificially increase the shear and bulk moduli on the sides of the footing for Case 3. The results from Case 2 are shown in Fig. 6.

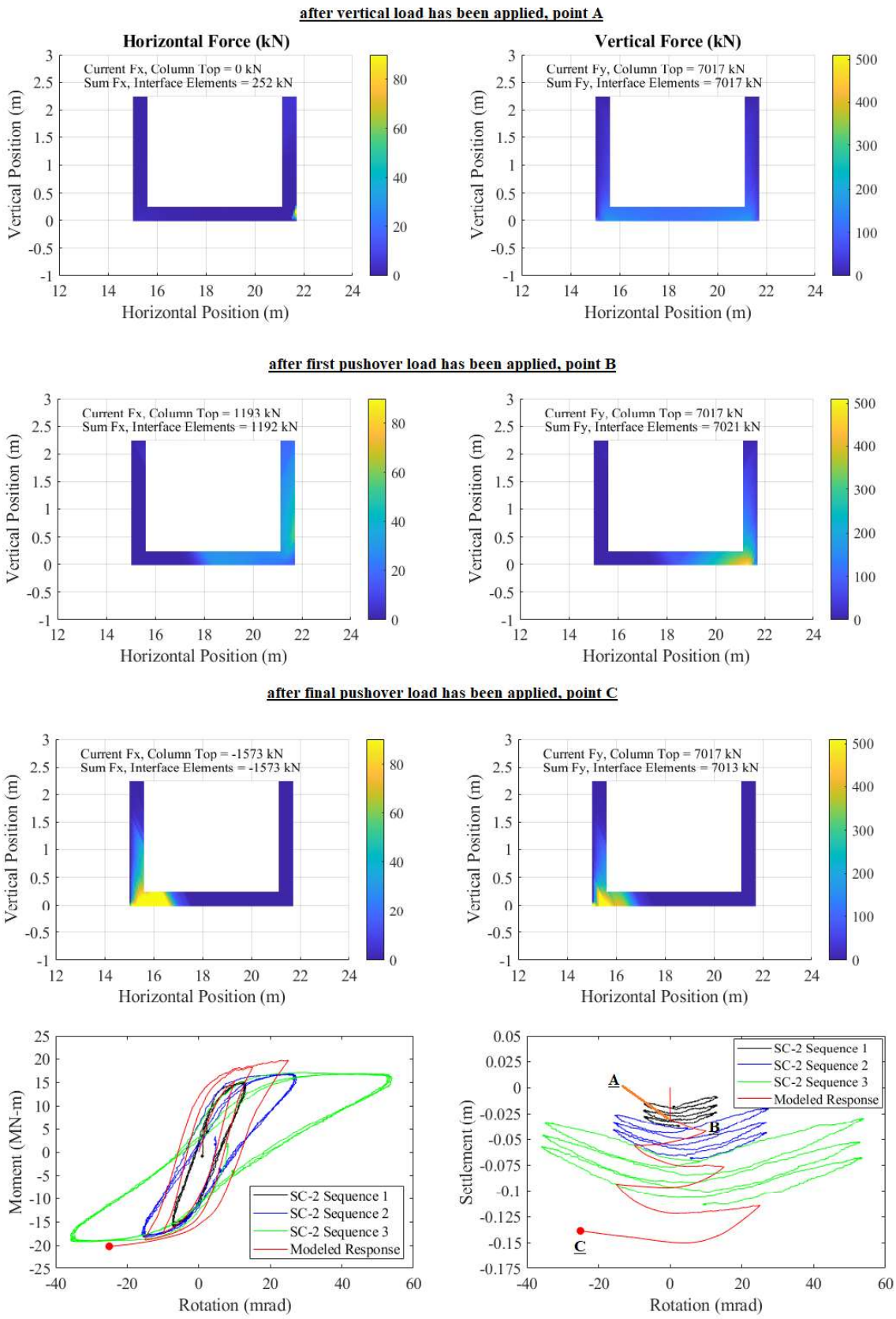

Fig. 6 – Case 2 model response against SC-2 slow cyclic test data [12]

At point A, the full vertical load has been applied and it is distributed evenly across the base of the footing. At point B, the first pushover half cycle has been applied and 1) the horizontal load is mostly resisted by passive pressure along the right side of the footing, and 2) the vertical load has migrated over to the bottom right corner. However, by the time a few load reversals have been applied, a gap has clearly developed between the footing side and the soil, because at point C, the horizontal load is now taken up almost entirely by friction on the bottom left corner. As shown in the bottom-most pair of plots in Fig. 6, the model matches the moment capacity well, but the numerically modelled footing settles much more than that in the SC-2 test.

This is true of another test (MC) used to validate the results, shown in Fig. 7. Two modeled responses are depicted in Fig. 7, one for Case 2 and another for Case 3. The load protocol for each was set to multiple cycles at the same rotation amplitude to better match the MC test sequence. The evolving load reaction across the sides and bottom of the footing for these results was observed to be similar to that depicted in Fig. 6. The model footing slides and settles much more than the test footing for both cases – the increased moduli in Case 3 have a limited effect. This suggests that the bulk of the moment capacity is derived from the soils beneath the base of the footing, and that once capacity is reached, substantial yielding is expected.

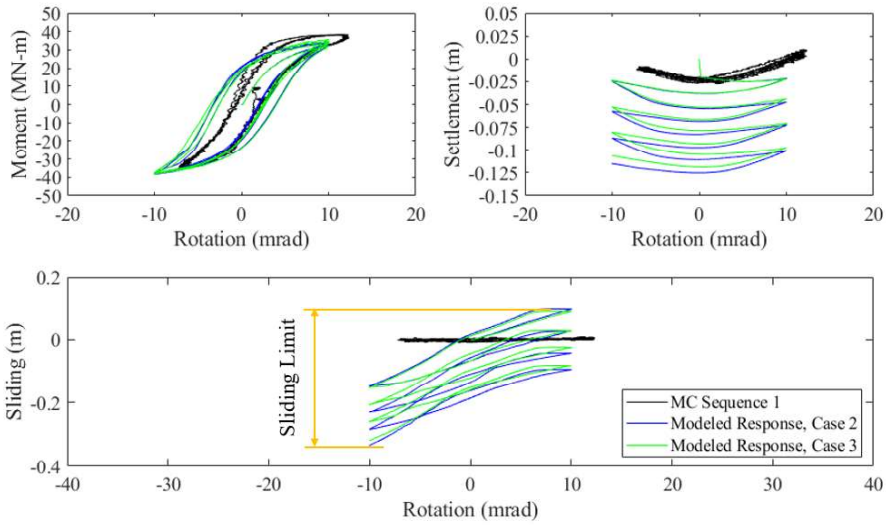

Fig. 7 – Case 2 and Case 3 model response against MC slow cyclic test data [12]

4. Numerical Model Parametric Study

Despite a lack of agreement between the modeled response and slow cyclic test data from [12], the model still has utility in examining relative effects of varying the ground improvement strategy. In addition to the three unimproved cases already mentioned, Cases 4 and 5 involve ground improvement via compacted stone – modeled by the PressureDependMultiYield material as for the sand. However, the shear modulus and friction angle of the stone have been increased to 200 MPa and 50°, respectively. The modulus is appropriate given the simple relationship presented in [27]. The stone for Case 4 is compacted in 7 vertical columns of 0.5 m-width and 5 m-length, evenly spaced across the length of the footing. The stone for Case 5 is instead compacted as a continuous mat across the length of the footing base. Its cross-sectional area is the same as the sum area of the columns in Case 4, and this yields a mat thickness of 1.7 m below the footing base.

Cases 6 and 7 involve ground improvement via soil-cement mixing similar to the methods described in [7, 8]. Because the mixture would exhibit clay-like behavior, it is modeled by the PressureIndependMultiYield material. Per field testing results reported in [7], a typical unconfined compressive strength of the mixture is 1.5 MPa. The cohesion input to the material model is half that, 750 kPa. The shear modulus is 150 MPa for a stiff clay [28]. The ground improvement geometry for Cases 6 and 7 is exactly the same as for Cases 4 and 5, respectively.

A summary of the parametric study results is shown in Table 2. Tabulated values represent four cycles of +/- 10 mrad rotation at the footing's center. The residual rotation is recorded during the last load cycle when the applied moment at the column top is zero. Energy dissipation ratio is directly proportional to the area within the moment-rotation curve and calculated per [12]. The footing does not slide for Case 1 because it is constrained laterally by a stiff spring, and because this reduces separation between footing and soil, the footing settles less than in Case 2 and 3. The increased stiffness on the sides of the footing for Case 3 has negligible effect on the results other than to reduce sliding slightly. The sand-cement mixture treatment increases energy dissipation over the stone treatment, although the residual settlement and rotation of the footing is greater for the mixture treatment. The sand-cement mat reduces sliding more than any other GI treatment strategy, consistent with the assertion in [5] that rocking induced soil yielding is mobilized within a *shallow* layer *underneath* the footing. Its utility is confirmed by Case 8 – where the mixture is additionally applied on the full sides of the footing extending laterally to the edge of the model. Even with this substantial increase in GI-treated area, the residual settlement and rotation are essentially the same as for Case 7, although the reduction in sliding for Case 8 would have beneficial implications for structural compatibility.

Table 2 – Parametric Study Results

CASE	Residual Settlement (mm)	Residual Rotation (mrad)	Sliding Limit (mm)	Energy Dissipation Ratio
No GI, Lateral Constraint (Case 1)	100	2.9	0	0.22
No GI, "Baseline" = MC (Case 2)	125	2.1	431	0.23
No GI, Modified Stiffness (Case 3)	119	2.7	408	0.24
Stone Columns (Case 4)	78	2.3	517	0.15
Stone Mat (Case 5)	87	2.4	537	0.15
Sand-Cement Columns (Case 6)	93	4.2	439	0.24
Sand-Cement Mat (Case 7)	86	3.0	199	0.26
Sand-Cement Mat+Sides (Case 8)	83	3.0	1	0.20

5. Numerical Model Application to Proposed Centrifuge Experiments

Because the numerical model predicts moment capacity well, it can be used as a first-order check for the magnitude of ground motion needed to dynamically load a footing in the centrifuge to its capacity. The test footing will be placed in a laminar container with flexible boundary conditions in the direction of shaking. These conditions are captured in the numerical simulation by enforcing equal displacements on the left and right sides of the model. A sample sinusoidal ground motion has been applied to the footings from Case 2 and Case 7 in the above table, and the dynamic loading simulation results are shown in Fig. 8.

6. Concluding Remarks

Rocking footings have been shown to increase energy dissipation and reduce damage to structures during seismic loading, and design methods are available in US and other guidelines, see for example ASCE 41. To further encourage their implementation, ground improvement techniques such as compacted stone and sand-cement mixing have been shown to reduce residual settlement and rotation of a heavily loaded footing. At present, the numerical simulations offer relative comparisons of these GI treatments. In the future, a closer examination of the cyclic yielding of the PressureDependMultiYield material model as well as a centrifuge testing program will provide stronger validation of the OpenSees numerical model.

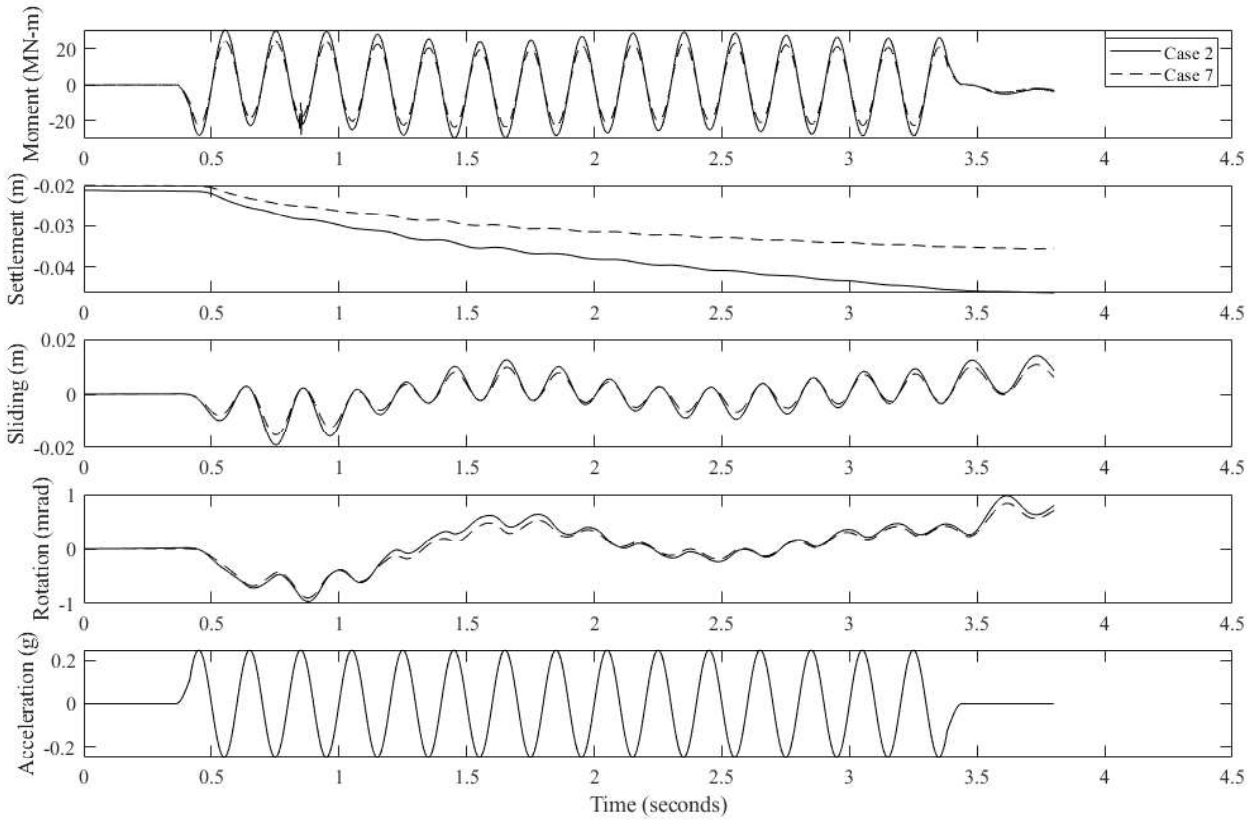

Fig. 8 – Dynamic loading simulation

6. Acknowledgements

This study was funded by the Pacific Earthquake Engineering Research (PEER) Center and their support is greatly appreciated. Findings of this work are those of the authors and do not necessarily represent PEER.

7. References

[1] Beck, JL and Skinner, RI (1973): The seismic response of a reinforced concrete bridge pier designed to step. *Earthquake Engineering & Structural Dynamics*, **2** (4), 343–358.

[2] Antonellis, G and Panagiotou, M (2014): Seismic Response of Bridges with Rocking Foundations Compared to Fixed-Base Bridges at a Near-Fault Site. *Journal of Bridge Engineering*, **19** (5), 1-14.

[3] Deng, L, Kutter, BL, and Kunnath, SK (2012): Centrifuge modeling of bridge systems designed for rocking foundations. *Journal of Geotechnical & Geoenvironmental Engineering*, **138** (3), 335–344.

[4] Adams, MT and Collin, JG (1997): Large model spread footing load tests on geosynthetic reinforced soil foundations. *Journal of Geotechnical & Geoenvironmental Engineering*, **123** (1), 66-72.

[5] Anastasopoulos, I, Kourkoulis, R, Gelagoti, F, and Papadopoulos, E (2012): Rocking response of SDOF systems on shallow improved sand: An experimental study. *Soil Dynamics & Earthquake Engineering*, **40**, 15-33.

[6] Malhotra, S (2007): Foundation considerations for seismic retrofit of bridges. *Ninth Canadian Conference on Earthquake Engineering*, Ottawa, Ontario, Canada. 26-29 June 2007.

[7] Arora, S, Shao, L, and Schultz, JM (2012): Wet Soil Mixing for Bearing Capacity, Liquefaction Mitigation, and Water Cutoff for Scour Protection for a New Bridge Abutment. *Grouting and Deep Mixing*, 575-584.

[8] Shao, L (2019): Soil Mixing Improvement for Bridge Abutment under Seismic Loads. *EERI 2nd Kenji Ishihara Colloquium Series on Earthquake Geotechnical Engineering*, San Diego, California. 23 August 2019.

[9] Pecker, A (2006): Enhanced seismic design of shallow foundations: Example of the Rion Antirion bridge. *4th Athenian Lecture on Geotechnical Engineering*, Hellenic Society of Soil Mechanics and Geotechnical Engineering, Athens, Greece.

[10] Hakhamaneshi, M, Kutter, BL, Gavras, AG, Gajan, S, Tsatsis, A, Liu, W, Sharma, K, Pianese, G, Kohno, T, Deng, L, Paolucci, R, Anastasopoulos, I, and Gazetas, G (2020): Database of rocking shallow foundation performance: Slow-cyclic and monotonic loading. *Earthquake Spectra*, **36** (2), 1585-1606.

[11] Gavras, AG, Kutter, BL, Hakhamaneshi, M, Gajan, S, Tsatsis, A, Sharma, K, Kohno, T, Deng, L, Anastasopoulos, I, and Gazetas, G (2020): Database of rocking shallow foundation performance: Dynamic shaking. *Earthquake Spectra*, **36** (2), 960-982.

[12] Deng, L and Kutter, BL (2012): Characterization of rocking shallow foundations using centrifuge model tests. *Earthquake Engineering & Structural Dynamics*, **41**, 1043-1060.

[13] Hakhamaneshi, M, Kutter, BL, Tamura, S, Gavras, AG, Liu, W, and Deng, L (2013): Rocking Foundations with Different Shapes on Different Soils. *10th International Conference on Urban Earthquake Engineering*, Tokyo, Japan. 1-2 March 2013.

[14] Hakhamaneshi, M, Gavras, AG, Wilson, DW, Kutter, BL, Liu, W, and Hutchinson, TC (2014): Effect of footing shape on the settlement of rectangular and I-shaped rocking shallow foundations. *8th International Conference on Physical Modelling in Geotechnics*, Perth, Australia. 14-17 January 2014.

[15] Sharma, K and Deng, L (2020): Field testing of rocking foundations in cohesive soil: cyclic performance and footing mechanical response. *Canadian Geotechnical Journal*, **57** (6), 828-839.

[16] Liu, W, Hutchinson, TC, and Stuedlein, AW (2015): Modeling of Foundation-Soil Systems Using Plane-Strain Elements. *6th International Conference on Earthquake Geotechnical Engineering*, Christchurch, New Zealand. 1-4 November 2015.

[17] Liu, W and Hutchinson, TC (2018): Numerical investigation of stone columns as a method for improving the performance of rocking foundation systems. *Soil Dynamics and Earthquake Engineering*, **106**, 60-69.

[18] Raychowdhury, P and Hutchinson, TC (2011): Performance of seismically loaded shearwalls on nonlinear shallow foundations. *International Journal for Numerical and Analytical Methods in Geomechanics*, **35**, 846-858.

[19] Gajan, S and Kutter, BL (2009): Contact Interface Model for Shallow Foundations Subjected to Combined Cyclic Loading. *Journal of Geotechnical and Geoenvironmental Engineering*, **135** (3), 407-419.

[20] NAVFAC DM7-2 (1986): Foundations & Earth Structures, Naval Facilities Engineering Command, Alexandria, Virginia.

[21] Bastidas, AM (2016): Ottawa F-65 Sand Characterization. Ph.D. Thesis, University of California-Davis.

[22] Alarcon-Guzman, A, Chameau, JL, Leonards, GA, and Frost, JD (1989): Shear modulus and cyclic strength behavior of sands. Soils and Foundations, **29** (4), 105-119.

[23] DeBeer, E (1965): Influence of the mean normal stress on the shearing resistance of sand. *International Conference on Soil Mechanics and Foundation Engineering*, Montreal, Canada.

[24] Bolton, MD (1986): The strength and dilatancy of sands. *Geotechnique*, **36** (1), 65-78.

[25] Elgamal, A, Yang, Z, Parra, E, and Ragheb, A (2003): Modeling of cyclic mobility in saturated cohesionless soils. *International Journal of Plasticity*, **19**, 883-905.

[26] Liu, W and Hutchinson, TC (2018): Numerical investigation of stone columns as a method for improving the performance of rocking foundation systems. *Soil Dynamics and Earthquake Engineering*, **106**, 60-69.

[27] Seed, HB and Idriss, IM (1970): Soil moduli and damping factors for dynamic response analyses. *Rep. No. EERC 70-10*, Earthquake Engineering Research Center, University of California, Berkeley.

[28] Yang, Z, Lu, J, and Elgamal, A (2008): OpenSees Soil Models and Solid-Fluid Fully Coupled Elements: User's Manual. Department of Structural Engineering, University of California, San Diego.

[29] Veletsos, AS and Meek, JW (1974): Dynamic Behaviour of Building-Foundation Systems. *Earthquake Engineering and Structural Dynamics*, **3**, 121-138.

